PROCEEDINGS, 51st Workshop on Geothermal Reservoir Engineering
Stanford University, Stanford, California, February 9-11, 2026
SGP-TR-230

Implementation of the World's First Greater than 300 °C Propped EGS Reservoir

Gabrijel Grubac[1], Wadood El-Rabaa[1], Alain Bonneville[1], Idris Ben-Fayed[1], Romar A. Gonzalez[1], Geoffrey Gullickson[2], Oswaldo Perez[3]

[1]Mazama Energy Inc. 2600 Network Blvd., Ste 550, Frisco, TX 75034

[2]Halliburton Company. 3000 North Sam Houston Parkway East, Houston, TX 77032

[3]KAPPA North America, Inc. 1500 CityWest Blvd; Suite 741, Houston, TX 77042

ggrubac@mazamaenergy.com

Keywords: EGS, stimulation, completion, superhot rock, diagnostics, fiber, tracers, fracturing, injector, producer, proppant

ABSTRACT

The deployment of Enhanced Geothermal Systems (EGS) at reservoir temperatures exceeding 300 °C presents unique technical challenges and opportunities for advancing geothermal energy production through the harnessing of higher enthalpy resources. Building on the successful completion and stimulation of the injector well in Phase I, this paper presents the design, testing, and field implementation of the producer well in the world's first propped EGS doublet >300°C at the Newberry Volcano, Oregon. A segmented stimulation strategy with a hybrid fluid design including crosslinked fluids and a hybrid completion in terms of wellbore to reservoir connection was developed for the producer well, incorporating field experience from the injector stimulation, real-time diagnostics and adaptive planning of treatment volumes. The approach integrates distributed temperature sensing (DTS) and distributed acoustic sensing (DAS) via permanent fiber optic installation in the injector well, enabling cross-well monitoring during stimulation of the producer. Tracers were deployed in the producer well to provide connectivity characterization, while micro seismic activity was monitored using multiple array set ups and fiber inferred DAS data. The Phase II program emphasizes the importance of iterative design, real-time connectivity, and advanced stimulation diagnostics to optimize fracture propagation and maximize the probability of connectivity between wells.

This work documents the methods, results, and lessons learned from Phase II completion and stimulation, culminating in the anticipated connection of the wells to enable circulation and heat harvesting. The findings provide critical insights for the advancement of next-generation EGS technologies at ultra-high temperatures and pave the path to de-risking technologies for superhot rock EGS development.

1. INTRODUCTION

1.1 Project Location and Geological Context

The project is located on the northwestern flank of Newberry Volcano, approximately 37 km (23 mi) south of Bend, Oregon, and roughly 16 km (10 mi) north of La Pine, within Deschutes County, central Oregon. The project area lies on federally managed land administered by the U.S. Bureau of Land Management (BLM), with surface oversight by the U.S. Forest Service, immediately adjacent to the Newberry National Volcanic Monument (Figure 1).

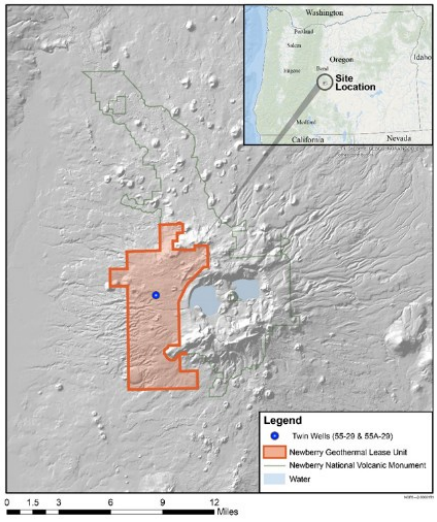

Figure 1: Location of the twin wells in Oregon

The geothermal leasehold encompasses approximately 50 km^2 (19.3 mi^2), consolidated into a unitized geothermal block to facilitate integrated exploration and development activities. This area contains multiple pre-existing geothermal well pads, deep exploration wells, temperature gradient boreholes, and seismic monitoring installations, all accessible via established gravel forest roads. The location was deliberately selected to balance high geothermal potential, existing infrastructure, and environmental and land-use compatibility.

Newberry Volcano is a broad shield-like composite volcano that has been active for approximately 600,000 years [*MacLeod et al.*, 1995]. The volcanic edifice is elliptical in plan view, measuring roughly 50 km by 30 km (31x18.5 mi), and rises to a maximum elevation of approximately 2,408 m (7900 ft) above mean sea level. Newberry Volcano occupies a geologically unique position at the intersection of three major tectonic provinces: Cascade volcanic arc; Columbia River Basalt Plateau and the Basin and Range Province.

The regional stress regime reflects a combination of north-south compression related to subduction processes and east-west extension associated with Basin and Range tectonics [*Flesch et al.*, 2000; *Priest*, 1990]. This stress configuration has contributed to faulting, dike intrusion, and fracture development within the volcanic edifice, all of which are critical controls on permeability and reservoir stimulation potential. The northwestern flank, where the project is located, is characterized by gently sloping terrain composed of overlapping basaltic and andesitic lava flows, volcaniclastic deposits, and localized silicic intrusions [*MacLeod et al.*, 1995]. Surface drainage is minimal due to the high permeability of young volcanic materials.

Four deep geothermal exploration wells (CEE 86-21, CEE 23-22, NWG 46-16, and NWG 55-29) have confirmed a predominantly conductive thermal regime, with minimal evidence of large-scale convective hydrothermal flow [*Waibel et al.*, 2014]. Previous injection and flow testing have demonstrated extremely low natural permeability, with injectivity values comparable to international hot-dry-rock projects [*Cladouhos et al.*, 2016]. Bulk permeability values on the order of 10^{-16} m^2 are several orders of magnitude lower than productive hydrothermal systems, confirming that reservoir stimulation is required to create economic flow pathways.

Lithologic data from deep geothermal wells indicate a bimodal volcanic composition, dominated by basaltic andesite and rhyodacite, with frequent intrusive bodies including granodiorite and felsic dikes and sills [*Waibel et al.*, 2014]. These intrusive units are particularly important from an EGS perspective because they tend to be mechanically brittle, fracture-prone, and thermally conductive, making them favorable targets for stimulation and long-term reservoir performance [*Cladouhos et al.*, 2016]. Decades of geothermal exploration have demonstrated that Newberry Volcano hosts one of the largest and hottest conductive geothermal anomalies in the western United States [*Blackwell et al.*, 1990]. Measured and extrapolated temperature data indicate temperatures above 315–320 °C at depths of ~2.7–3.0 km (~1.7-1.9 mi) and projected temperatures exceeding 400 °C below ~4 km (2.5 mi) [*Frone et al.*, 2014] placing the system among the most promising superhot EGS targets in North America [*Bonneville et al.*, 2018].

2. Injector stimulation learnings and producer well planning

The EGS project included a re-completion and stimulation of the existing 55-29 well, planned as the injector of the well pair. The workover implied the pulling of the upper 7” slotted liner and completing the well with 7” x 4.5” cemented casing. Once re-completed, the well was stimulated utilizing abrasive jetting, wireline-based perforations and high viscosity friction reducers in 6 treatments. The stimulation was carried out in variable lithologies including basalt, andesite and granodiorite (Grubac et al., 2025). Upon finalizing the injector well stimulation in January 2025, an analysis ensued including fiber related data, tracer diagnostics, stimulation pressure responses and the inferring of engineered reservoir volume. A flowback operation of the injector well was implemented in February 2025 and the samples analyzed for nano tracers. The results showed a signature of each tracer pumped during the stimulation of 55-29 in all stages, indicating physical communication from reservoir to 55-29 wellbore. (Grubac et al., 2025)

With the above in mind, a design analysis for producer well placement included: stimulation design and generated geometries, sensitivity to fracture initiation and orientation along the bottom segment of the reservoir and connectivity probability between the wells.

A 2010 borehole televiewer operation (Davatzes & Hickman, 2011) indicated a N2.3° +-17° maximum horizontal stress component SHmax orientation. Utilizing this information as well as the fiber DAS inferred information giving N16° ± 5° (see section 3), the assumed SHmax was determined to be N9°+/-7° and the placement of the producer well accounting for tolerance in stress direction was designed as shown in Figure 2. Variable simulations on stimulation design including volumetrics, fluids, rate and proppant types and concentrations were performed to better understand extent and quality of propped fracture length distribution. With the inferred geometries from the injector well, the producer simulations were then coupled along with well placement and stress orientation tolerance to understand connectivity scenarios between wells, and their respective stimulations stages as shown below.

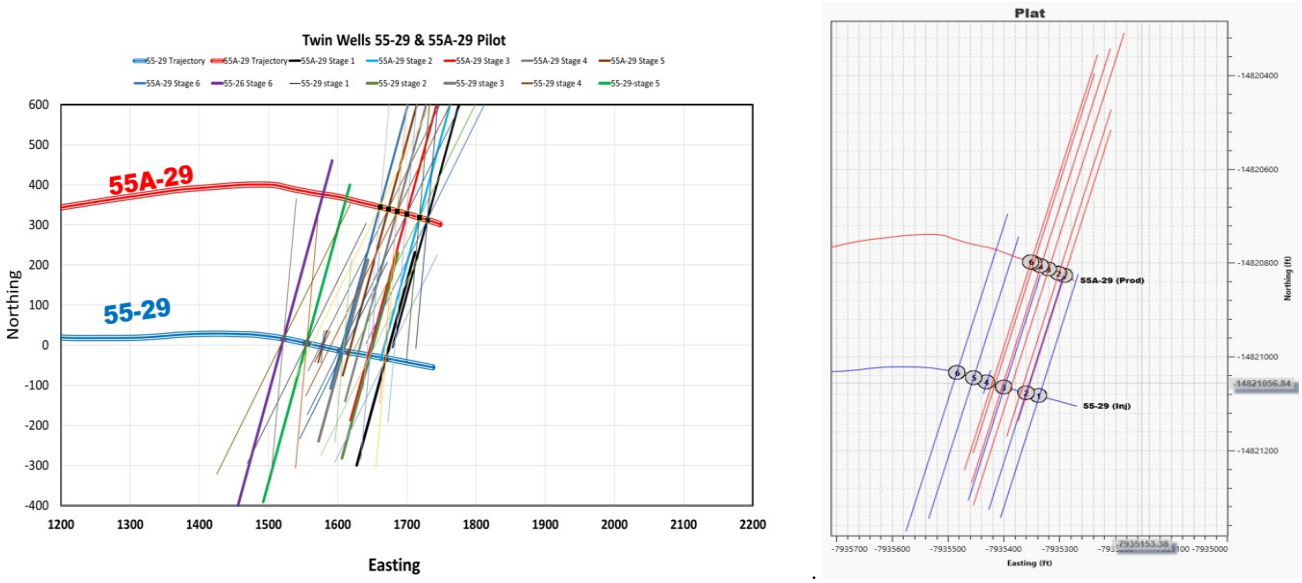

Figure 2: Simulation and alignment of fracture orientations in connecting the injector and producer wells (map view)

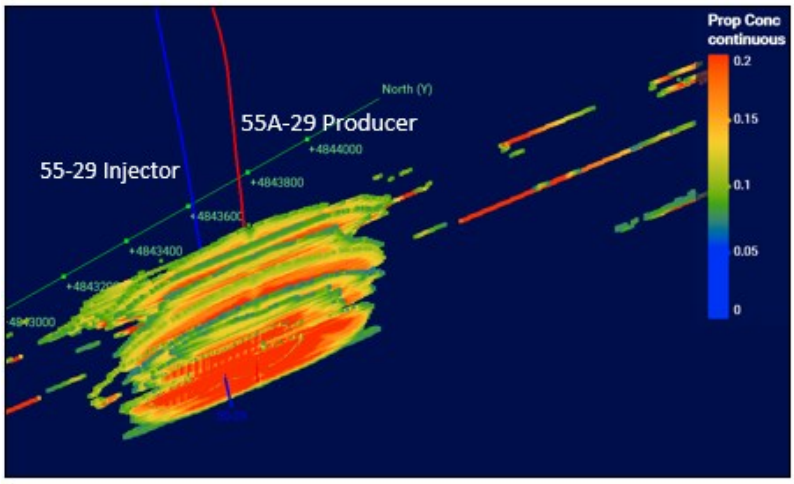

Figure 3: Modelled iterations of fracture extensions from producer to injector well

In all cases, the designed propped length exceeded 80m and proppant areal distribution satisfied the requirements in terms of intended conductivity and geometry (Figure 3). Multiple modelling iterations were performed to finalize the well spacing decision. The well spacing of 90-100m was confirmed and relayed to the drilling team for placement.

Below was the guiding stimulation approach focus for the producer 55A-29:

1. **Create fracture widths ≥2mm**
    a. The ability to enhance fracture width and allow for improved conductivity for flow efficiency
    b. With lithology being a limiting factor along with native mechanical properties, the approach would include fluid system and pumping rate sensitivities
2. **Mitigate fluid loss considering secondary system leak-off**
    a. Injector stimulation diagnostics indicated low fluid efficiencies in zone of stimulation. This required attention in terms of maximizing chances of effective stimulation treatment in the producer and avoid proppant packing prematurely
    b. Application of increased quantities of micro proppants through the stages based on respective diagnostic test response

3. **Enhance perforation erosion**

    a. Lower perforation frictions and enable an easier fracture generation process

    b. Application of 100mesh in respective stages that would help with erosion and further aid leak-off

4. **Increase pre-pad for cooling**

    a. Injector stimulation temperature data helped optimize operations in the injector

    b. Sensitivities in stimulation design ran with pre main treatment to enable cooling of the rock in ways that would not aggressively degrade the viscosity of the fluid carrying the proppant. A more rigorous and detail-oriented approach will be required for the future once subsurface data is more populated with calibrated properties

The mud log of 55A-29 during drilling was analyzed and stage picks for producer stimulation picked based on the below criteria and learnings from the injector well stimulation:

- Target granodiorite for improved stimulation efficiency
- Target deeper segments to maximize temperature contact
- Target segments to align with 55-29 fractures and TVD and increase chances of fracture connection and disturbed rock volume
- Pick a basalt stage to replicate 55-29 approach and better understand fracability
- Basalt stimulation being possible but with increased risk and need for tailoring stimulation approach

2. Producer well drilling and placement

55A-29 was drilled to a total measured depth of 10,200 ft, using a staged well construction approach comprising four primary hole sections. The primary objectives of the well were to execute the drilling program to successfully parallel the existing well 55-29, prove and de-risk technologies required to optimize field development, enable hydraulic stimulation and fracture connectivity between the twin wells, and demonstrate the viability of an enhanced geothermal system (EGS) in a ~331°C reservoir through sustained heat harvesting.

Drilling commenced with the 26” top-hole section, extending from surface to approximately 1,100 ft MD, through highly fractured and vesicular volcanic formations characterized by severe lost circulation. Multiple drilling approaches, including downhole hammers, PDC bits, and multiphase fluid systems, were deployed. The section was successfully completed meeting casing objectives and providing a stable foundation for accurate well placement in deeper sections.

The subsequent 17½” intermediate section, drilled from approximately 1,100 ft to 3,700 ft MD, focused on rapid depth advancement while maintaining trajectory control to ensure parallelism with well 55-29. PDC bits and heavy, high-inertia bottom-hole assemblies delivered rates of penetration significantly exceeding offset wells.

The well then transitioned into the 12¼” build and tangent section, extending from approximately 3,700 ft to >9,000 ft MD, where directional accuracy and drilling dynamics were critical. Initial constraints related to motor availability were mitigated through iterative optimization of BHA design and drilling parameters, resulting in improved stability and sustained drilling performance.

The 8½” production section was drilled from approximately 9,000 ft to TD at 10,200 ft MD, representing the deepest and highest-temperature interval. PDC bits delivered exceptional performance, achieving rates of penetration two to three times higher than offset wells. Downhole temperatures remained within tool limits, validating thermal management practices and confirming the feasibility of drilling deep volcanic formations using conventional drilling and measurement technologies

2.1 Trajectory design and directional placement

Well trajectory planning was driven by stimulation objectives, including required inter-well spacing, stimulation volume, and acceptable pressure drop. As this was a first-of-its-kind application, prior experience provided limited guidance. Lateral separation between the two wellbores was therefore defined directly from stimulation design constraints.

Pad constraints required the twin producer (55A-29) to be drilled south of the existing 55-29 well, although the optimal parallel orientation was north of the existing well. Temperatures exceeding 330 °C eliminated the use of rotary steerable systems due to tool survivability, expected drilling dysfunction, operational support requirements, and limited steering reliability in noisy basalt formations. Consequently, 55A-29 was drilled using a positive displacement motor (PDM), with trajectory control achieved through sliding and rotating. The well was drilled vertically to 1,320 m TVD, then kicked off toward the northwest (Figure 4). Placement prioritized minimizing survey error while maintaining the required parallel length and toe spacing relative to the existing producer. Curves were designed with a low dogleg severity of 2.5°/30 m, terminating before the 7-in liner section and resulting in a tangent inclination of 27°. The tangent section was drilled close to plan using small corrective slides to maintain inclination and azimuth.

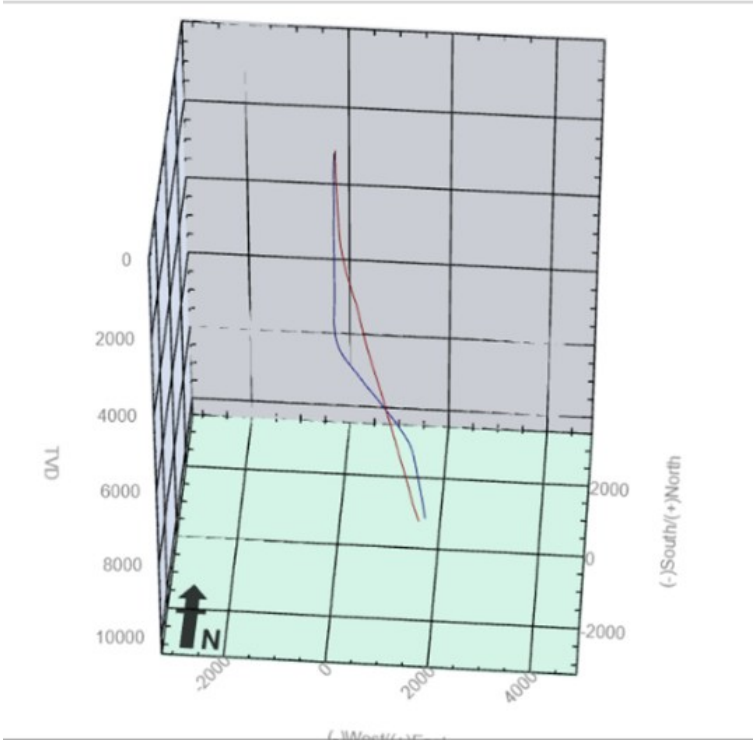

Figure 4: Trajectory designs for 55-29 (red) and Producer (blue)

To realize the notional thermal, hydraulic, and stimulation objectives the drilling objectives became:

- Manageable torque and Drag
- Vibration management
- Tool survivability
- Survey Error Management
- Dogleg Severity vs Contact Length

Ultimately, these questions reduce to whether a well can be drilled in these hard volcanics that have previously been hydro sheared. The build rates of 2.5°/30m in volcanics was confirmed as realistic at temperature with abrasive rock and vibration limits based on the offset reports of 55-29 from 2008. This became the basis of the build and turn rates for the trajectory. The BHA design revolved around the PDM and PDC selected strategy. The PDM-PDC choice was for performance and engineered specifically for lithology in Newberry. This left stabilization design. This was a bespoke approach developed with the stabilizer vendor. The torque and drag modeling with the selected BHA and trajectory showed the drill pipe selected was within the operating limits even with the high friction factors historically experienced in volcanic drilling.

Thermal management was an important element of the drilling process and specifically surveying as these measurements depend on electronics. The key to understanding when and how to deploy surveying program was based on the understanding of the wells thermal legacy, usage of insulated drill pipe, staging protocols, and mud coolers. This means that the surveying and resurveying had to be done at specific depths. To help answer this question, uncertainty survey growth and separation factors were calculated for the known trajectory of the actual producer and planned producer. Traditional view on this subject is from the perspective of anti-collision. separation factors based on uncertainty growth. For the stimulation team an engineered reservoir volume was necessary and prescribed wellbore spacing was key. Well spacing constrained the drilling path.

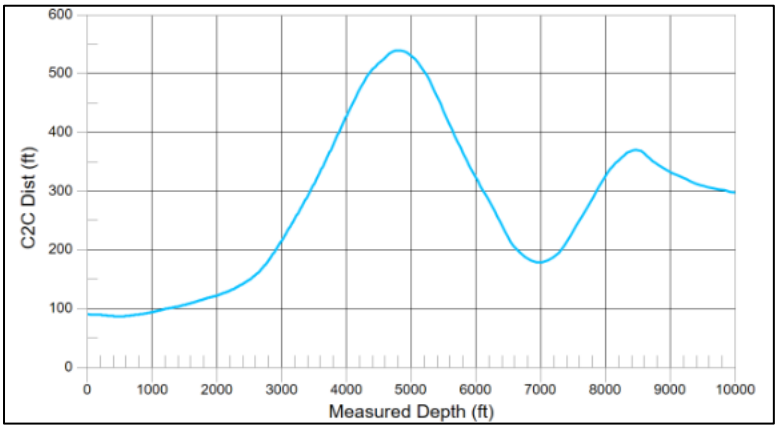

Figure 5: Theoretical well center to center separation in feet for 55-29 and 55A-29

Figure 5 shows the planned and perfect outcome. Focusing on separation factors would be misleading as it's a ratio of centre-to-centre distance to sum of ellipsoid radii. The planning process had to focus on survey quality and error models. Each surveying tool planned for the Newberry location had their specific error models used in the trajectory planning. With MWD quality at high temperature being a challenge, thermal modeling became a fundamental challenge to wellbore placement, as previously stated. The magnetic interference of the lithology and direction chosen was addressed by building the uncertainty ellipses in the planning phase and in real time with every survey. How the uncertainties were handled was based on the outcomes of the minimum and maximum distances between the two wells at the beginning and toe of the parallel sections.

Figure 6 shows the uncertainties in wellbore placement with the planned wellbores in planar view. It shows the placement uncertainty could be as large as 30% of the intended separation. It also shows at which depths that a reduction in the error of uncertainty (EoU) yields the greatest impact for trajectory planning. This is the roadmap necessary to enable real time decision making.

Well placement had 95% confidence that the positional uncertainty ellipse remained within the defined target corridor and maintained the required wellbore separation between the pairs. The decision-making framework for the operations team and developed by the planning team needs to compare target window to the uncertainty ellipse. In other words, if the ellipse is equal to the target window, there is either need for a different approach or a different well placement tolerance.

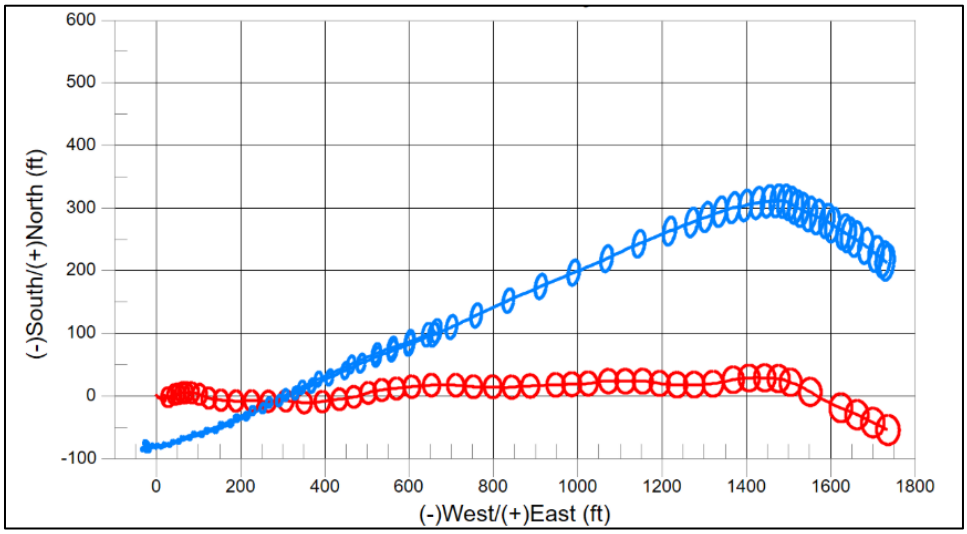

Figure 6: Uncertainty in wellbore placement prior to Mazama Energy operations on 55-29 (red) and 55A-29 (blue)

The understanding of the wellbore's thermal legacy and staging needs kept the downhole tools that we needed working. It was understood that thermal management was necessary to keep the tools reading but, what measurements dictate our responses on surface depended on the dysfunction. The same downhole dysfunction that reduces steerability also increases noise in measurements and bias. This amplifies positional uncertainty. The issue of micro-tortuosity through repeated corrective steering isn't the subject now, although it is a corollary. When the MWD traffic lights are being transmitted, it's important to review the issue being measured and how it translates to trajectory placement.

- Stick–slip: the bit repeatedly stalls and then suddenly accelerates. Surface RPM can look steady while downhole RPM swings significantly.

- Bit bounce: a periodic axial vibration that leads to loss of weight transfer, with impacts as the bit re-contacts bottom.
- Whirl: the bit/BHA rotates eccentrically; can be forward whirl or more damaging backward whirl.
- Coupled vibrations: in hard, heterogeneous volcanics, torsional + lateral + axial can reinforce each other

Each dysfunction has different adverse steering responses for motors with bent housing. The torsional and lateral modes cause the downhole tool face to oscillate even if surface indications show that it is being held. The consequence of this is a wellbore with inconsistent building and turning. In execution phase this means that the same planned slide can give different dogleg depending on whether the bit is cutting smoothly or intermittently stalling/bouncing.

While sliding, the axial and torsional modes are critical for directional control. However, the same downhole dysfunctions that reduce trajectory control also affect MWD surveys. MWD surveys are computed from accelerometers for inclination and magnetometers for azimuth. Vibration degrades both measurements.

- Axial/lateral shocks add “non-gravity” accelerations.
- Magnetometer corruption caused by lateral vibration and whirl can introduce noise; additionally, the magnetic interference exacerbates the incorrect azimuth reading.
- Torsional oscillation issues: if downhole RPM surges, the measurement window may not represent the assumed steady state; tool face and azimuth calculations become noisier.

The normal modus operandi is to have everything stationary to take these measurements. As the bottomhole environment exceeded 300C the above was not an option. So, thermal modeling allowed the understanding on how to enable these measurements. Therefore, during the drilling process the below metrics were used for trajectory control. This illustrates how the exact wellbore placement is a multi-faceted and highly integrated solution.

- Downhole dynamics channels track stick-slip severity, axial, and lateral indicators.
- Tool face changes with standard deviation during slides or tool face oscillation amplitude.
- ROP efficiency: sudden ROP drops correlated with torque spikes or vibration flags.

The link between drilling performance and on-bottom ROP can be made and the practical mitigation during operations can be seen as

- Bit aggressiveness, gauge length, stabilizer placement, motor bend/RSS settings.
- WOB/RPM management to avoid resonant bands
- Consistent hydraulics

Solving the well placement issue holistically not only located the pair within six feet of its desired trajectory to a depth of about 10,000 feet but also increased bit longevity, up to 2760ft in basalt and granodiorite and ROPs of 76-100ft/hr in the same hard abrasive volcanic rocks.

2.2 Core retrieval and encountered proppant

A core recovered on July 5th, 2025 (Figure 7), showed definitive proof of connection between injector and producer considering the proppant particles that were found in the cored sample. The core had been retrieved at a depth coinciding with Stages 5 and 6 in the producer and injector. The coring process and proppant encountered:

- Confirmed displacement of proppant of ~305ft center to center between wells (93m)
- Carry significant implication in obtaining physical proof of proppant displacement and its effects on future well spacing decisions for enhanced heat harvesting through stimulation
- Hydraulic fracture simulators predicted fracture half-length of 91 to 110 m for Stage 5 and stage 6 pumped from 55-29 further giving confidence in the modelling work and implication from running sensitivities for producer well design

Figure 7: 55A-29 core image showing proppant particles

3. Diagnostics and seismic monitoring

3.1 Diagnostics and Monitoring During Injection

Micro seismic monitoring plays a critical role throughout both the development and operational phases of EGS projects. During stimulation, the detection and analysis of micro seismic events provide a real-time window into subsurface processes, enabling the characterization of fracture networks, disturbed volumes, and reservoir geometry. These data are essential for evaluating the effectiveness of stimulation strategies, identifying fluid pathways, and informing decisions regarding well placement and injection protocols. Beyond reservoir characterization, micro seismicity is also central to managing seismic risk.

Three seismic monitoring means (two surface networks and one DAS optical fiber in well 55-29) were deployed at Newberry site during the stimulations of the twin wells 55-29 and 55A-29.

3.2 Newberry Permanent Seismic Network operated by Lawrence Berkeley National Laboratory (LBNL)

The seismic monitoring array deployed at the site is an integral part of the induced seismicity mitigation protocol (ISMP) implemented at Newberry. The array consists of eight sensors installed in “shallow” boreholes, reaching depths of up to 300 meters below the surface (Figure 8). This network is also supplemented with nearby stations operated by the University of Washington (UW via Pacific Northwest Seismic Network; PNSN) and USGS via the Cascades Volcano Observatory (CVO). Arrays of nodal seismometers have been installed in July 2025 to supplement the data from borehole sensors.

All data are streamed in near real time to LBNL, where they are processed in real time to detect, locate, and estimate the magnitudes of seismic events associated with the injection operations. The results are monitored on site by the stimulation team and displayed on the Mazama Energy website for public access (Seismicity Tracker available at https://mazamaenergy.com/newberry/).

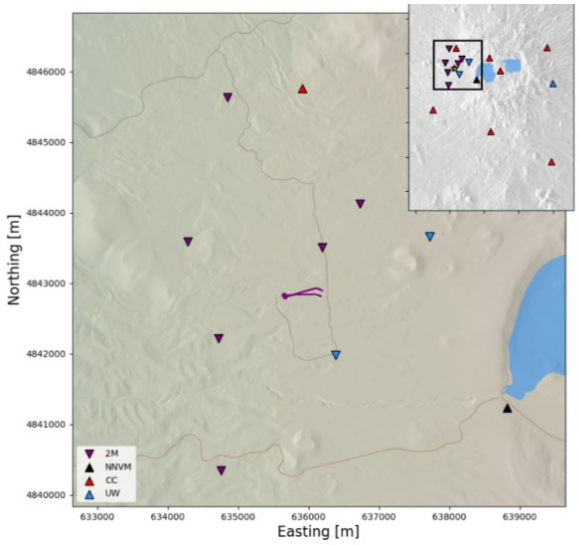

Figure 8: Wider-area seismic network surrounding the Mazama seismic network. The LBNL-Mazama network is shown in deep purple, the CVO network in red, and the PNSN network in blue. Well 55-29 and 55A-29 are shown in purple trajectories. The black triangle (NNVM) corresponds to the strong motion sensor.

During the stimulation of well 55-29, eleven events were detected by the LBNL-Mazama network but only two are most likely related to stimulation activity. During the stimulation of well 55A-29, the network detected 35 events, but visual review of the signals revealed that most of them were likely noise related to operations on the surface and did not exhibit the characteristics of subsurface seismic events. At least seven of these events were associated with lightning activity in the vicinity.

3.3 Fiber-optic DTS/DAS

Distributed Acoustic Sensing (DAS), Distributed Temperature Sensing (DTS), and microseismic monitoring were conducted in the 55-29 observation well before, during and after the stimulation treatments were performed in the two wells. The permanent fiber was installed outside casing in the 55-29 observation well to an end-of-fiber (EOF) depth of 2705 m (8,875 ft). The installation consisted of both single-mode fiber for DAS/strain measurements and multimode fiber for DTS measurements.

Unlike the surface seismic network, the DAS has recorded 150 events clearly related to the two stimulations. The recorded microseismic cloud aligns with an azimuth of approximately N16°E ± 5°, consistent across both stimulations (Figure 9).

The microseismic event clouds are clustered above their respective stage locations, indicating preferential upward growth (Figure 10). However, the clouds also show lateral propagation, indicating that fractures are extending horizontally as well, enlarging the EGS footprint. Inter-stage microseismic activity was sparse suggesting low reservoir activity.

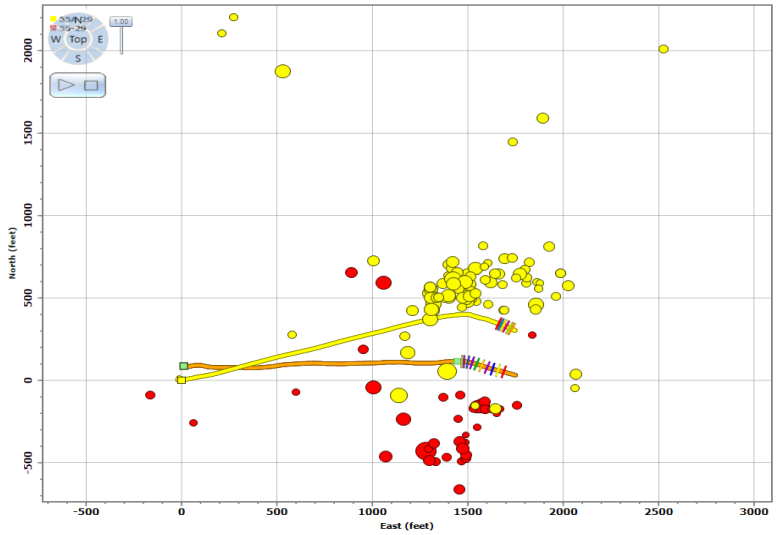

Figure 9: Map view of microseismic events induced by stimulation of well 55-29 (red disks) and by stimulation of well 55A-29 (yellow disks). The disk size is proportional to event magnitude.

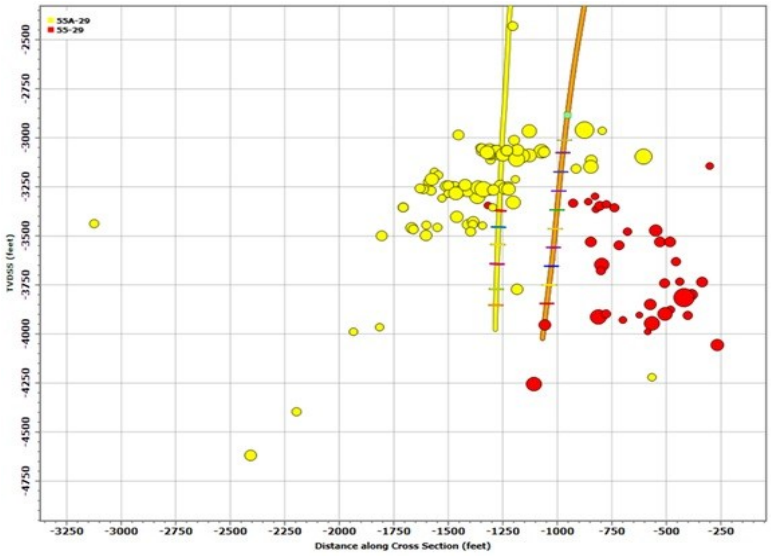

Figure 10: North-South cross-section showing microseismic events induced by stimulation of well 55-29 (red disks) and by stimulation of well 55A-29 (yellow disks). The disk size is proportional to event magnitude.

The strain/thermal response in the fiber well during the communication test, while pumping continued in 55A-29 (stages 4,5), is a strong indicator of hydraulic connectivity. This suggests that the fracture network created during stimulation reached the offset well, allowing pressure and fluid transmission. (Figure 11). Strain and temperature changes on 55-29 coincide with real time stimulation of producer 55A-29 and performed flow tests on the injector well 55-29.

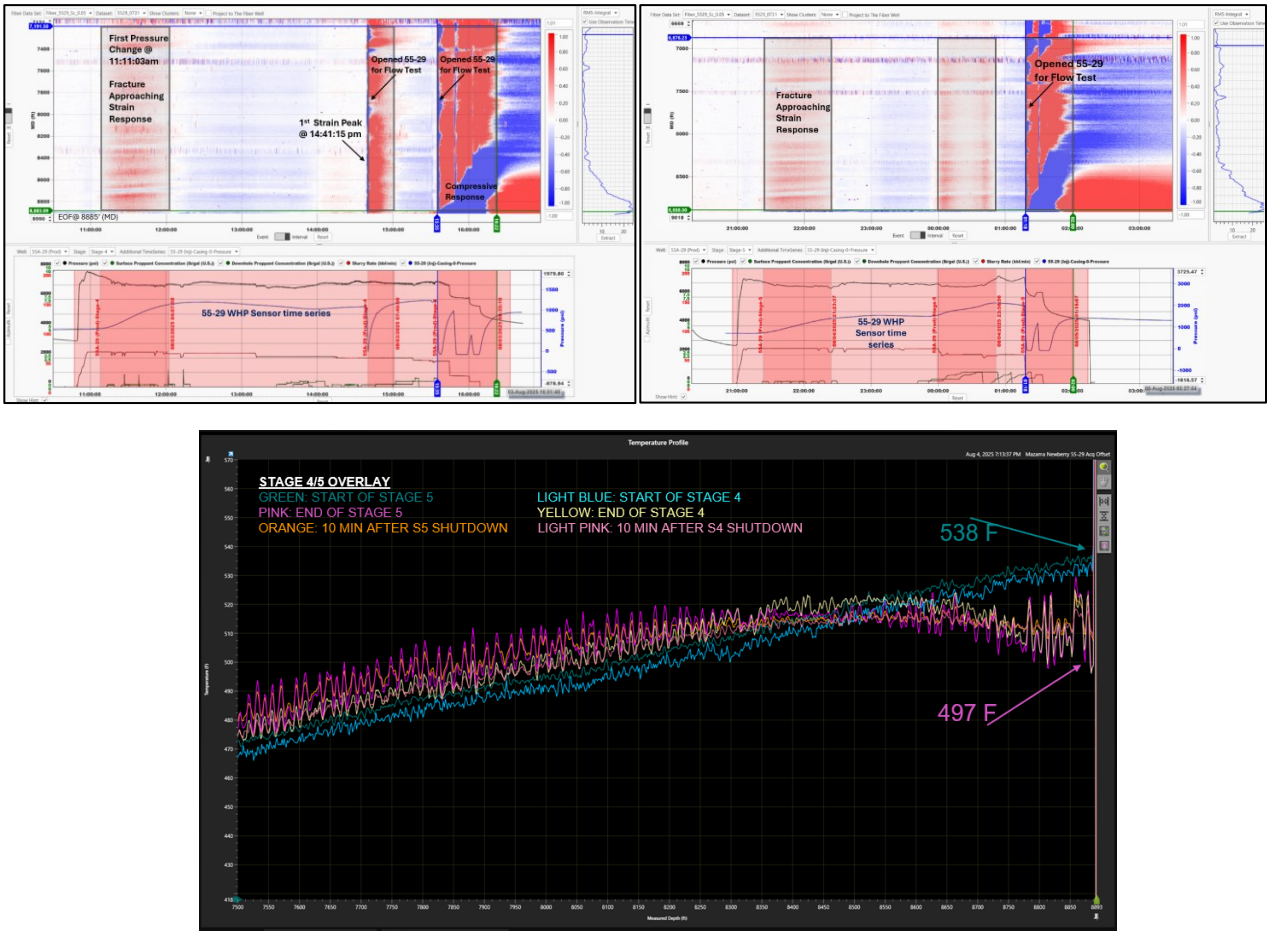

Figure 11: Injector strain (top left - Stage4, top right - Stage 5) and temperature changes on fiber (bottom image) while pumping Stages 4 & 5 in 55A-29 and flow testing 55-29. Temperature is in degrees Fahrenheit and measured depth in feet

3.4 Surface seismic array.

During the stimulation of 55A-29, a surface array was deployed covering approximately 28.5 km^2 (11 mi^2), consisting of 14 arms and 1,357 stations, each equipped with six geophones per channel. Sixteen events were recorded by this array with moment magnitudes between –1.7 and –0.8. They were also located by the DAS with similar depths confirming the validity of the overall location determination.

The dominant trend of the cloud is North–South, and the primary source mechanism is oblique dip-slip with dip angles of 45°–60°. Three-dimensional lineaments exhibit steep North–South dips and shallow East–West dips. Nodal planes derived from auto MTI align with these lineaments and regional surface features used for stress analysis. Fractures striking subparallel to SHmax and dipping 55°–70° are the most critically stressed, while steeply dipping fractures in the same orientation show the greatest dilation tendency. The stress regime deduced from a careful analysis of focal mechanisms is characterized by SHmax ranging from 4°–10° and a Phi value of 0.50–0.58, indicating a normal faulting environment, compatible with the orientation of the cloud deduced from the DAS observations and with a previous study using BHTV showing a direction of N2.3 +/- 17º.

Main observation from the seismic monitoring

All three monitoring methods have shown that the stimulation of wells 55-29 and 55A-29 induced a few, very small seismic events. In total, only 150 microseismic events were recorded, most of them only detected by the DAS fiber deployed to a depth of 2705 m (8,875 ft) in well 55-59, very close to the stimulation stages. It should be also noted that no seismic activity linked to the EGS reservoir was detected during the months between the two stimulations and since August 2025, which is also quite remarkable.

4. Wellbore to reservoir connection

The producer had been completed utilizing a hybrid approach in terms of sleeve and wireline conveyed perforations for the stages above Stage 1. A sliding sleeve was successfully installed at 10,063 ft measured depth (MD) in Stage 1 of well 55A-29. The sleeve was positioned across a granodiorite interval, as interpreted from mud logging data. Sleeve opening was successfully achieved using a rig-based, drill-pipe-conveyed mill, confirming mechanical integrity and operability of the system at depth. Following installation, two injection tests were conducted to evaluate reservoir response. The pressure and rate behavior indicated a more complex interaction with the formation, deviating from conventional flow regimes. Analysis of the injection data indicates the presence of a secondary leak-off mechanism, implying increased fluid loss into the formation beyond classical fracture leak-off behavior. Fracture fluid efficiency decreased notably between the two tests, dropping from approximately 44–58% in Test 1 to 26–28% in Test 2, consistent with increased leak-off and formation complexity. The injection tests are presented in Figure 12.

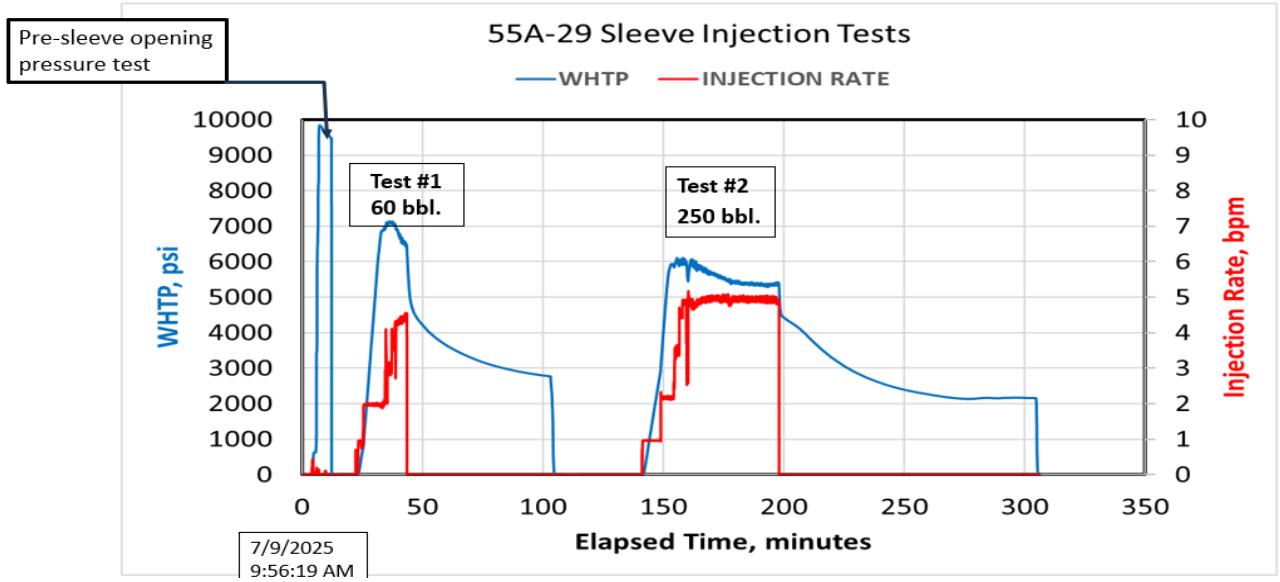

Figure 12: 55A-29 Stage 1 injection tests

4.1 Newberry 55A-29 Fluid System Development

Building from the key diagnostic evidence from the Newberry 55-29 project, a hybrid HVFR/Crosslinked fluid system was selected for the Newberry 55A-29 treatment. The previous testing on High Viscosity Friction Reducer (HVFR) (Grubac et al., 2025) did not require further investigation, but a battery of tests was needed for several anticipated formation cooldown conditions to effectively support fracture modeling and optimum proppant schedule development.

A dry Carboxymethyl Hydroxypropyl Guar (CMHPG) utilizing a Zirconium solution was selected as the fundamental base polymer and downhole crosslinker to meet the modeled rheological competency needs up to a temperature of 150 deg C (300 deg F) without requiring gel stabilizer additives (Halliburton, 2018). Additional additives included:

- Non-alkaline basic solution to ensure proper high pH compliance
- Borate low temperature crosslinker to facilitate effective proppant transport at the high-shear perforation interface
- Glutaraldehyde biocide used to treat the bulk water storage system ensuring competent gel hydration stability

All additives were selected with a focus on environmentally friendly chemistry given the sensitive wellsite location in Central Oregon, USA volcanics. From preliminary fracture modeling efforts, a 40lb/Mgal CMHPG base loading was selected for testing. All other additives were iterated using that polymer concentration to create the most stable fluid system possible using field source water. After the additive concentrations and operating fluid system conditions were determined, pressurized rheology testing was completed at 66-204 deg C (150-400 deg F) in 27 deg C (50 deg F) increments (Fig. 13).

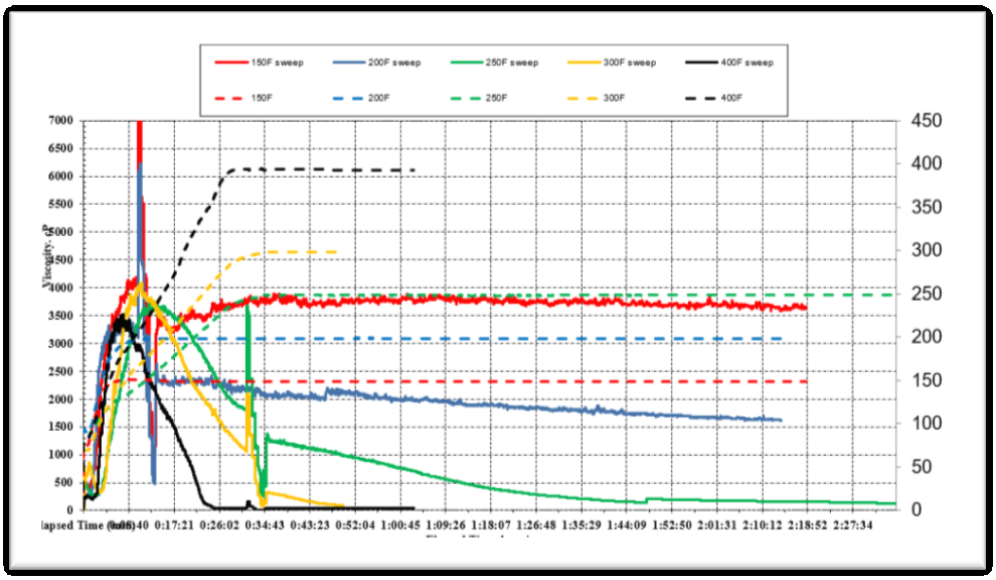

Figure 13: 55A-29 Baseline Rheology Testing – 66-204 Deg C (150-400 deg F) – y-axis is viscosity in cP and x-axis is time in hr:min:sec

Power Law Modeling of fluid values n′ (flow behavior index) and k′ (flow consistency index) were obtained through established shear rate-stress relationship sweep testing practices (Melton et al., 1957). For this testing, one sweep was executed immediately when the fluid sample reached its target test iteration temperature. The sweep was executed at the shear rates of 10-20-40-100-200-511s-1. Before and after the sweep test, a shear rate of 40s-1 was held constant during sample heat up and viscosity stability monitoring.

The results were processed and utilized in the fracture modeling package in developing the total material balance and most effectively conductive proppant schedule. The n′-k′ results are presented in graphical and numerical format in Fig. 14.

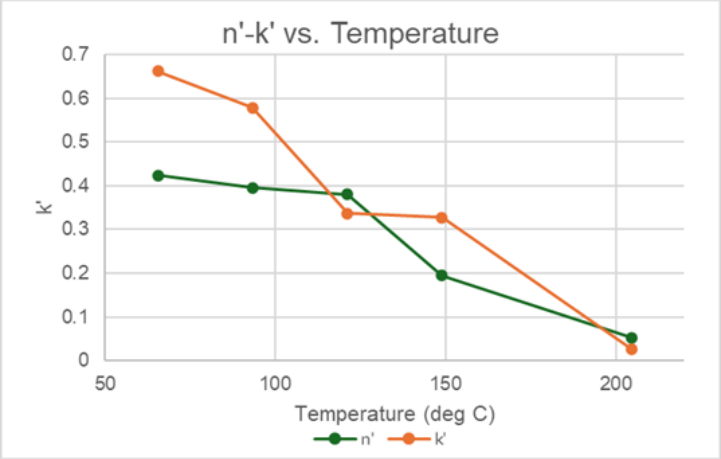

Temperature (°C)	Temperature (°F)	Sweep @ Temp n'	Sweep @ Temp k'
66	150	0.4236	0.6623
93	200	0.3957	0.5788
121	250	0.3797	0.3369
149	300	0.1949	0.327
204	400	0.0527	0.0272
		Shear Rate = s^{-1}	
		Shear Stress = (lb/ft^2)	

Figure 14: 55A-29 n'-k' vs. Temperature / Shear Rate Sweer Testing

4.2 ***Newberry 55A-29 Stimulation Surface Operations***

Because a plug and perforate stimulation isolation and formation access system was selected for the multiple intervals of propped fracture stimulation, a conventional surface rig-up for a hybrid HVFR/Crosslinked fluid system was mobilized. A total of 24,000 HHP of high-pressure pumps were mobilized to meet a maximum designed service requirement of 60bpm at 11,200psi. This pumping equipment factored an appropriate operational contingency excess that needed to accommodate for extreme remote operations a minimum of 48 hours from a local high pressure pumping service yard. Additionally, independent dry gel polymer and proppant blending equipment, proppant handling and passive/active storage, injection and flowback surface manifolding, coiled tubing well intervention equipment, various downhole wireline and coiled tubing tools, bulk Aboveground Storage Tanks (AST), water transfer with progressive high rate filtering, a working tank battery, field fluid system lab, and a data acquisition command center was required to service a 24hr operation extremely far from existing well stimulation operations infrastructure.

The to scale surface representation of the total stimulation and well intervention equipment required across multiple service providers and operator supplied equipment is presented in Figure 15.

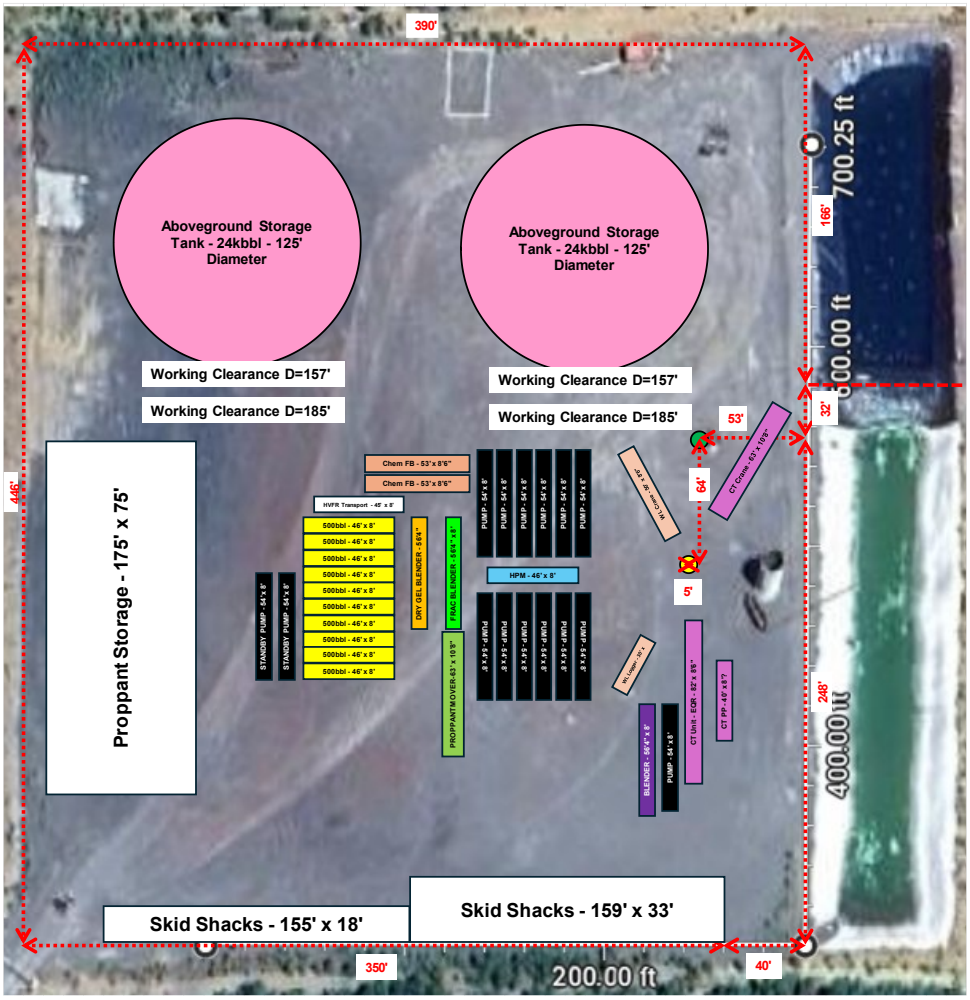

Figure 15: To Scale Surface Stimulation and Well Intervention Equipment Rigup

5. Pressure interference and well to well connection

Below is a summary of the interactions encountered between the producer 55A-29 and injector 55-29 during the stimulation treatment of 55A-29. It is important to note that real-time field supervision and analytics were critical in characterizing the connections during the stimulation and applying analytical approach in terms of volumetrics changes and diagnostics during pumping. The below was further proof in confirming physical connection between the wells. The approach in analysis [Haas et al., 2025], consisted in:

1. Identify first pressure interactions.
2. Understanding the main first response attributes driving pressure interactions.
3. Analyze pumping parameters affecting first response signals.
4. First response attributes are useful to optimize completion designs:
    a. Time to observe first response
    b. First response differential pressure (dP)
    c. Volume injected to observe FR

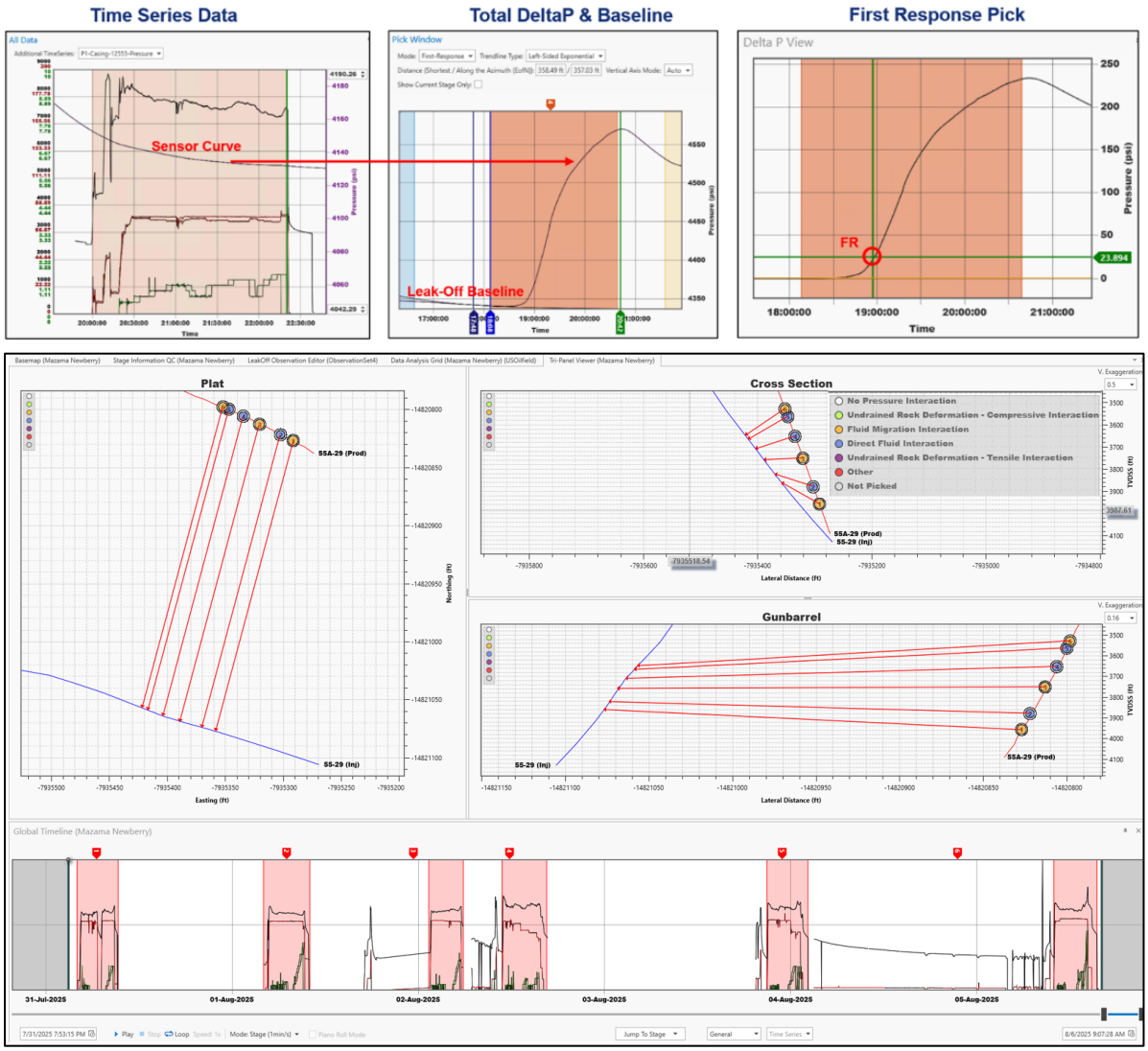

Figure 16: Pressure interference approach to analysis on a stage-by-stage basis (Top). Discretized FDI events between producer and injector consisting mostly of "direct fluid interactions" and "fluid migration" events.

Table 1: Summary of FDI offset pressure responses in injector well (55-29) during stimulation of producer well (55A-29)

55A-29 Stage Number	FDI Type	First Response Δ Time to Pick [min]	First Response Δp	First Response Volume to Pick [bbl]	First Response Surface Proppant to Pick [lb]	Length of pressure change (min)	Total Δ Pressure [psi]	Nanotracer signature in circulation test
1	Fluid Migration Interaction	78.6	11.5	3101.8	13316.4	318.2	114.4	Yes
2	Direct Fluid Interaction	58.7	18.6	1326.0	1293.3	335.7	182.6	Yes
3	Fluid Migration Interaction	61.5	9.7	2830.9	12759.2	270.4	104.7	Yes
4	Direct Fluid Interaction	28.9	65.9	1386.7	1452.4	278.5	687.7	Yes
5	Direct Fluid Interaction	40.8	142.7	2038.2	2886.1	233.7	1408.0	Yes
6	Fluid Migration Interaction	34.7	29.3	1812.1	3015.6	268.3	296.6	Yes

6. Tracers – confirmed well to well connection and circulation

Ultrahigh-resolution nanoparticle tracers and chemical tracers were deployed to evaluate connectivity and flow behavior within the engineered reservoir volume. During circulation testing following the drilling and stimulation of the twin wells, fluid samples were collected over time at the wellhead flowline and sent for laboratory analysis. Two independent tracer providers and analytical methodologies were used to improve confidence in the results, enabling interpretation of downhole surface area connectivity and providing diagnostic insight into stimulation effectiveness. Both results coming from the nano tracer analysis as well as chemical tracers indicate physical connectivity between the wells and proved connection in the engineered reservoir volume.

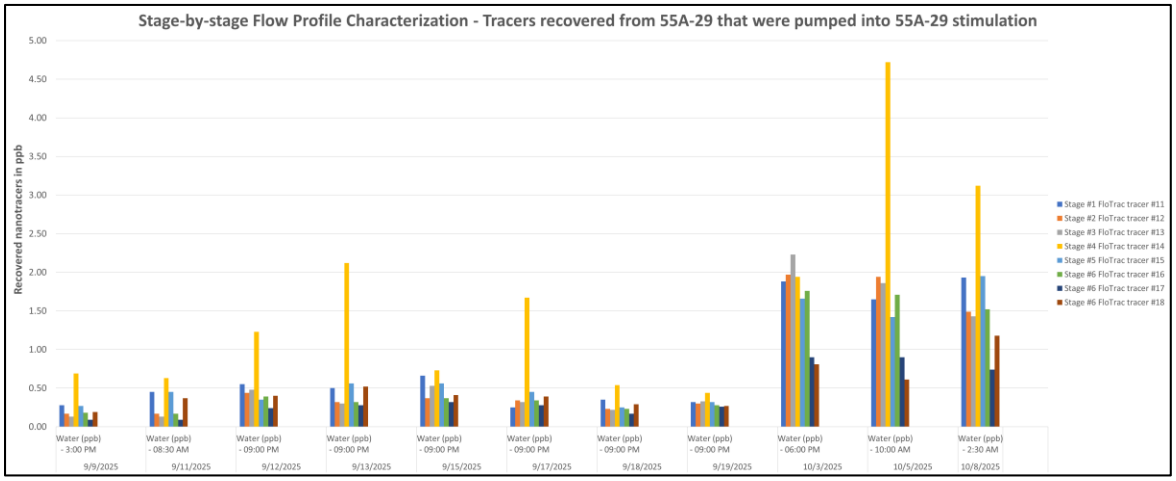

Figure 17: Nano tracers pumped in producer stimulation recovered in the flowback samples of the producer

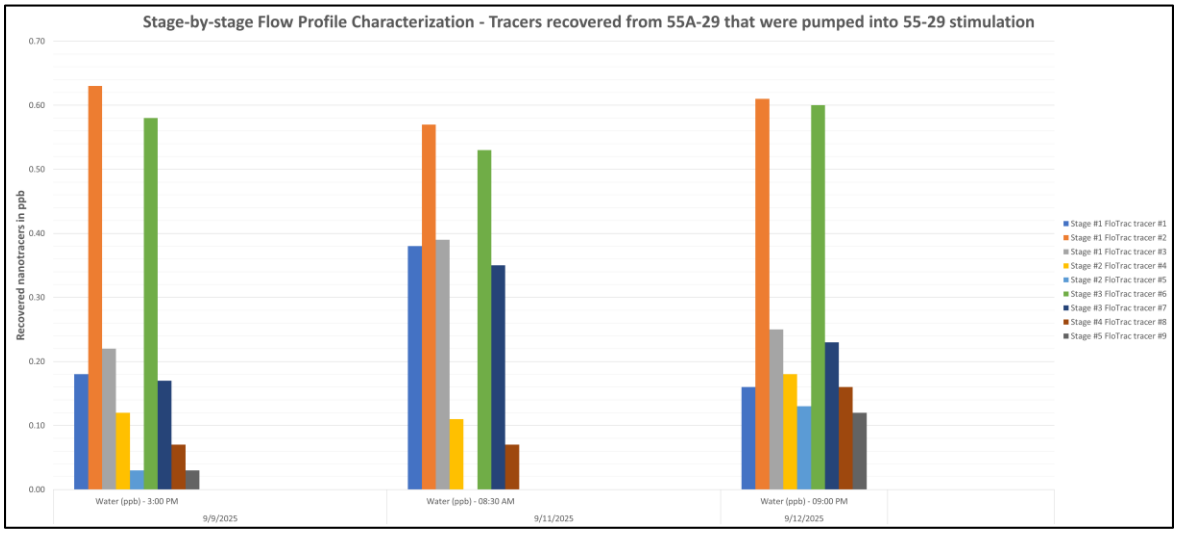

Figure 18: Nano tracers pumped in injector stimulation recovered in the flowback samples of the producer

The individual test for chemical tracer X was injected during a 10-day circulation test. Due to curve shape observed, fast breakthrough was detected. Double peak observed corresponds to volume estimations and timings suggesting second peak is a result of reinjection of tracer. Ultimately, the connectivity between the wells has been once more proven through detection of chemical tracer pumped in the injector and recovered into the producer well. The below information is further used to characterizing direct and indirect connected volumes and future implications in de-risking EGS development.

Table 2: Circulation test tracer test summary

Parameter	*Description / Notes*	*Value*	*Units*
Mass Recovered	Fraction of injected tracer mass recovered at producer	13	%
Average Residence Time	How long the tracer mass spent moving within the connected flow network	27	hours

Swept Volume	Estimated reservoir volume contacted by the tracer	195	bbl
First Arrival of Tracer	Time after injection when tracer was first detected	9.5	hours
Volume on First Arrival	Cumulative injected volume at first arrival (pipe volumes removed)	141	bbl
Peak Arrival of Tracer	Time after injection when tracer concentration peaked	12.5	hours
Volume on Peak Arrival	Cumulative injected volume at peak arrival (pipe volumes removed)	321	bbl
Residence Time at Peak Arrival	Effective residence time corresponding to peak tracer response	7.5	hours

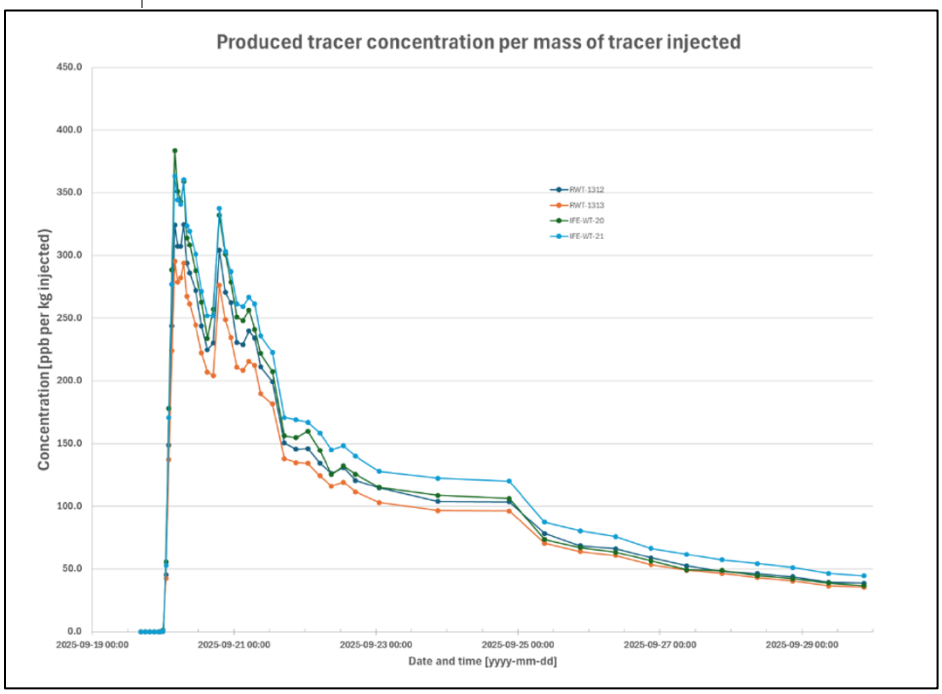

Figure 19: Produced chemical tracer concentration per mass of tracer injected – samples at producer well 55A-29

7. CONCLUSIONS

The creation of an EGS reservoir between 55-29 & 55A-29 wells has demonstrated the implementation of injector re-entry, stimulation, producer drilling, producer stimulation and final connection and circulation. This successful pilot project has paved the way to a commercial project at Newberry and pushing forward the superhot rock development status in the world. Here are the most noticeable results:

- Completion of first ever >300 °C propped EGS twin-well pilot with confirmation of hydraulic connection and circulation to harvest heat.
- First hybrid fluid stimulation design and application including high viscosity friction reducers and crosslinked systems for enhanced proppant transport and engineered rock volume.
- First successful sleeve installation and application for propped stimulation >300°C.
- Utilization of fiber technology to better understand thermal dynamics, confirm connection between wells and apply stimulation oil and gas technologies in >300°C geothermal environments.
- Microseismicity analysis has confirmed SHmax azimuth, ultimately aiding future horizontal wells placement for superhot rock EGS.
- No induced microearthquake with magnitude >0 detected and operations completed successfully
- Successful deployment of advanced diagnostics including nano tracers and chemical tracers and confirming connection and circulation between injector and producer wells.

The next steps include reservoir thermal equilibration and circulation characterization and quantification. The outcome of this work will help inform and pave the way forward for future superhot rock horizontal well planning and maximizing chances of efficient connection and circulation for commercial power production.

REFERENCES

Blackwell, D. D., J. L. Steele, M. K. Frohme, C. F. Murphey, G. R. Priest, and G. L. Black (1990), Heat flow in the Oregon Cascade Range and its correlation with regional gravity, Curie point depths, and geology, Journal of Geophysical Research: Solid Earth, 95(B12), 19475–19493, doi:https://doi.org/10.1029/JB095iB12p19475.

Bonneville, A., T. T. Cladouhos, S. Petty, A. Schultz, C. Sørlie, H. Asanuma, G. Ó. Friðleifsson, C. Jaupart, and G. de Natale (2018), The Newberry Deep Drilling Project (NDDP) workshop, Sci. Dril., 24, 79–86, doi:10.5194/sd-24-79-2018.

Cladouhos, T. T., S. Petty, M. W. Swyer, M. E. Uddenberg, K. Grasso, and Y. Nordin (2016), Results from Newberry Volcano EGS Demonstration, 2010–2014, Geothermics, 63, 44–61, doi:https://doi.org/10.1016/j.geothermics.2015.08.009.

Davatzes, N., and S. Hickman (2011), Preliminary Analysis of Stress in the Newberry EGS Well NWG 55-29, *Transactions - Geothermal Resources Council*, *Vol. 35*, 323–332.

Flesch, L. M., W. E. Holt, A. J. Haines, and B. Shen-Tu (2000), Dynamics of the Pacific-North American Plate Boundary in the Western United States, Science, 287(5454), 834–836, doi:doi:10.1126/science.287.5454.834.

Frone, Z., A. Waibel, and D. Blackwell (2014), Thermal Modeling and EGS Potential of Newberry Volcano, Central Oregon., paper presented at Thirty-Ninth Workshop on Geothermal Reservoir Engineering, Stanford University, February 24–26.

Grubac, G., Gullickson, G., Bonneville, A., Brand, P., Goloshchapova, D., Dunham, E. M., Khan, M., Cuthill, D., Shokanov, T. A., Gibson, C., Palisch, T., Hopp, C., and Nakata, N., 2025. *Enhanced geothermal system propped stimulation >300 °C: From design to implementation—Phase I*. Proceedings, SPE Annual Technical Conference and Exhibition, Houston, Texas, USA

MacLeod, N. S., D. R. Sherrod, L. A. Chitwood, and R. A. Jensen (1995), Geologic map of Newberry Volcano, Deschutes, Klamath, and Lake Counties, Oregon. USGS Miscellaneous Geologic Investigations Map I-2455, US Geological Survey.

Priest, G. R. (1990), Volcanic and tectonic evolution of the Cascade volcanic arc, central Oregon, Journal of Geophysical Research: Solid Earth, 95(B12), 19583–19599.

Waibel, A. F., Z. S. Frone, and D. D. Blackwell (2014), Geothermal Exploration of Newberry Volcano, OregonRep., Medium: ED; Size: 147 p. pp, United States.

Haas, G., Perez, O., and Artus, V. (2025). *Integration of multidisciplinary fracture diagnostics for the evaluation of well completions in unconventional plays: Application to the HFTS-2 dataset*. Proceedings, SPE/AAPG/SEG Unconventional Resources Technology Conference, Houston, Texas, USA, June 9–11, Paper URTEC-4254269-MS, https://doi.org/10.15530/urtec-2025-4254269

Halliburton (2018). Sirocco Fracturing Service, Halliburton Technology Bulletin, SMA-18-004

Melton, Leonard L., and Calvin D. Saunders. "Rheological Measurements of Non-Newtonian Fluids." *Trans.* 210 (1957): 196–201. doi: https://doi.org/10.2118/716-G